

# Band filling dependence of the electrical transport of $\text{Nd}_{1-x}\text{A}_x\text{TiO}_3$ ( $\text{A} = \text{Ca}, \text{Sr}$ and $\text{Ba}$ )

S. Das\*, A. Poddar, B. Roy

Saha Institute of Nuclear Physics, 1/AF, Bidhannagar, Calcutta 700064, India

Received 27 October 2003; received in revised form 14 November 2003; accepted 14 November 2003

## Abstract

We are here reporting the results of the studies of X-ray, electrical resistance ( $R$ ) and thermoelectric power (TEP,  $S$ ) on  $\text{Nd}_{1-x}\text{A}_x\text{TiO}_3$  ( $\text{A} = \text{Ca}, \text{Sr}$  and  $\text{Ba}$ ) over a wide temperature range as a function of 3d band filling  $n$  ( $=1-x$ ). Depending upon the levels of band filling all the compounds studied show both insulating as well as metallic behavior thereby exhibiting a metal–insulator (M–I) transition. The filling level at which M–I occurs varies with the size of the divalent alkaline earth ions A. In the correlated metallic phase resistance data scales well with  $T^2$  suggesting that electron–electron scattering plays a major role governing the conduction mechanism. Analysis of the  $T$ -linear part of the TEP measurement reveals that the occurrence of the metal–insulator transition is due to the enhancement of the effective mass of the carriers. © 2003 Elsevier B.V. All rights reserved.

**Keywords:** Titanate; Metal–insulator transition; Resistivity; Thermopower

## 1. Introduction

Recently, intensive studies on the electronic properties of the 3d transition metal compounds with perovskite related structure have revealed a number of intriguing features [1,2] of highly correlated electron system. Because of the strong electron–correlation effect and resultant carrier localization, most of these compounds undergo a metal–insulator (M–I) transition as a function of temperature, carrier concentration, bandwidth and so on [2]. In the Zaanen–Sawatzky–Allen (ZSA) scheme [3], insulating properties arising from the strong correlation between d electrons can be categorized into two classes: Mott insulators (MI) and charge transfer insulators (CTI). In Mott insulators the minimum charge gap is formed between the d electron states i.e., the upper and lower Hubbard bands whereas in CT insulators, the gap is formed between the ligand (e.g., oxygen) p state and the unoccupied d-like upper Hubbard band. According to the ZSA scheme, the parent compounds for cuprate superconductors with  $3d^9$  configuration have been assigned to CT-type insulators whereas some light transition metal oxides (e.g.,  $\text{V}_2\text{O}_3$ ) with localized d-electron states are the Mott insu-

lators. A Mott–Hubbard insulator can be transformed to a correlated metal by enhancing the one-electron transfer interaction and hence reducing the relative strength of the electron correlation effect ( $U/W$ , where  $U$  is the on-site Coulomb repulsion and  $W$  is the one-electron bandwidth of the conduction band) with application of external pressure such as observed in  $\text{V}_2\text{O}_3$  [4] and  $\text{PrNiO}_3$  [5] or, with modification of the chemical composition as employed in  $\text{RNiO}_3$  (R being the rare-earth ion) [6]. The M–I transition induced by changes of the bandwidth of the conduction band is termed as bandwidth controlled insulator–metal transition. In addition to the phase change associated with an opening or, closing of the Mott-type or, CT-type gap due to variation of  $U/W$  at a fixed integer valence of the constituent metal element, there exists another type of insulator–metal (I–M) transition induced by changes of the band filling of the conduction band. This is termed as carrier doping or, filling controlled I–M transition where the electronic process is qualitatively different from the case of conventional doped semiconductors with weak electron correlation. A typical example of the doping-induced I–M transition is that observed in layered cuprate compounds where drastic changes of electronic structures and properties have been observed with variation of the effective valence of Cu or, through filling of the Cu–O related band. It is to be mentioned here that the perovskite structure compounds are quite suitable for filling

\* Corresponding author.

E-mail address: sailen@cmp.saha.ernet.in (S. Das).

control since their structure is very tough in withstanding chemical modification on the perovskite A-site. In the filling controlled systems as the I–M phase change is approached from the metallic side many unconventional phenomena have been unravelled, for instance charge and spin ordering [7], colossal magnetoresistance [8,9], antiferromagnetism [10], ferromagnetism, high temperature superconductivity [11–13] and so on. Recently an intense attention has been devoted to the perovskite-type system  $R_{1-x}A_xTiO_3$  (R being a trivalent rare earth and A is a divalent alkaline earth) where both the bandwidth and the band filling can be chemically controlled [14–16]. The end member  $RTiO_3$ , where the R atom is in the  $3d^1$  electron configuration, is a Mott insulator irrespective of the rare-earth R. Here the one-electron band width ( $W$ ) of the conduction band can be varied [17] by changing R. On the other hand, substitution of the trivalent R ion by the divalent A ion decreases the number of electrons per Ti site or, the band filling  $n$  ( $=1-x$ ) and drives the system metallic. In the metallic regime of  $R_{1-x}A_xTiO_3$  many of the characteristic fingerprints for Fermi liquid, such as  $T$ -squared resistivity,  $T$ -independent Pauli-like susceptibility and the  $T$ -linear coefficient of the specific heat have been observed [14,18]. Additionally the carrier effective mass is found [19] to be critically enhanced as the I–M transition is approached from the metallic side indicating a strong role of electron correlation for the M–I transition. Apart from the recent extensive studies, however, not so much has been known about the doping induced I–M transition in the Mott–Hubbard systems. Moreover, there is scarce report for the thermoelectric power on this system although this experiment is a sensitive probe of the degree of itineracy of the carriers and an investigation of the thermoelectric response in the regime where large mass enhancement has been observed is highly desirable. In view of this we have undertaken a systematic study of the electrical transport and thermoelectric power (TEP,  $S$ ) measurement of the perovskite-type solid solution system  $Nd_{1-x}A_xTiO_3$  ( $A = Ca, Sr$  and  $Ba$ ) where one can control the effective Ti valence from  $3^+$  ( $x = 0$ ) to  $4^+$  ( $x = 1$ ) or band filling while essentially maintaining the original lattice structure. In the parent  $NdTiO_3$  insulator partial substitution of  $Nd^{3+}$  sites with  $A^{2+}$  ions drives the phase change from a Mott–Hubbard insulator to a correlated metal. We observed a transitional behavior from the doped Mott insulator to the narrow band metal with increasing  $x$  (or decreasing the band filling  $n$ ).

## 2. Experimental

$TiO_2$  powder was prefired at  $1000^\circ C$  for 24 h. Polycrystalline  $ATiO_3$  ( $A = Ca, Sr$  and  $Ba$ ) were prepared by heating the mixture of  $TiO_2$  and  $ACO_3$  ( $A = Ca, Sr$  and  $Ba$ ) in air at  $1000$ – $1200^\circ C$  for 48 h with intermediate grindings and pelletization. The structure of  $ATiO_3$  was confirmed by X-ray diffraction. Neodymium oxide ( $Nd_2O_3$ ) was heated at  $1000^\circ C$  in air for 12 h prior to use. The stoichiomet-

ric mixture of prefired  $ATiO_3$ , prefired  $Nd_2O_3$  and  $Ti_2O_3$  were mixed homogeneously and pressed into pellets. The pelletized mixture was then melted in an arc furnace in argon atmosphere with repetitive turnings. To obtain a single phase the samples were remelted several times with intermediate grindings. The samples thus prepared were found to be brittle and preserved in a dessicator purged with argon gas to avoid oxidation.

The crystal structure and the phase purity of the samples were checked by powder X-ray diffraction with  $Cu K\alpha$  radiation using a Philips APD 1877 X-ray diffractometer. Due to the irregular shape of the samples precise determinations of the resistivity was not possible. Temperature dependence of the electrical resistance and thermopower were measured using methods as described elsewhere [25]. The thermopower of the samples was measured using a differential technique where a temperature gradient is created across the sample and the voltage developed between the hot and cold ends of the thermocouple formed by the sample and Cu wires is measured. The details of the set up and measurement technique have been reported earlier [20].

## 3. Results and discussions

### 3.1. X-ray diffraction

Fig. 1 depicts a representative X-ray diffraction pattern of  $Nd_{1-x}A_xTiO_3$  ( $A = Ca, Sr$  and  $Ba$ ). Analysis of the X-ray data of the compounds shows that the samples studied are single phase. The Ca- and Sr-doped  $NdTiO_3$  shows perovskite crystal structures with orthorhombic distortions (GdFeO<sub>3</sub>-type) throughout the concentration range studied. The X-ray pattern of  $Nd_{1-x}Ba_xTiO_3$  can be well fitted with cubic symmetry. Thus it is found that the incorporation of the small size  $Ca^{2+}$  ( $r_{Ca} = 1.48 \text{ \AA}$ ) and  $Sr^{2+}$  ( $r_{Sr} = 1.58 \text{ \AA}$ ) ions produces an orthorhombic distortion throughout the whole concentration range whereas the largest Ba ion ( $r_{Ba} = 1.75 \text{ \AA}$ ) produces cubic symmetry.

### 3.2. Resistivity

In Figs. 2–4 we show the temperature dependence of the normalized resistance  $R_n$  ( $=R/R_{300}$ ) of  $Nd_{1-x}A_xTiO_3$  ( $A = Ca, Sr$  and  $Ba$ ). For the  $Nd_{1-x}Ca_xTiO_3$  ( $x = 0.1$ – $0.8$ ) system Fig. 2 shows that the normalized resistance  $R_n$  of the  $x = 0.1$  sample increases with the decrease of temperature similar to that of a semiconducting sample. The upturn in  $R_n$  at low temperature may originate from the effect of carrier localization. The nature of the  $R_n(T)$  curves of all samples with  $x = 0.2$ – $0.8$  are quite similar. With decreasing temperature starting from room temperature  $R_n$  decreases like a metallic sample and then after crossing a certain temperature it decreases very slowly with lowering of temperature. The metallic nature of  $R_n$  is consistent with earlier reported results [21]. Thus samples with low filling

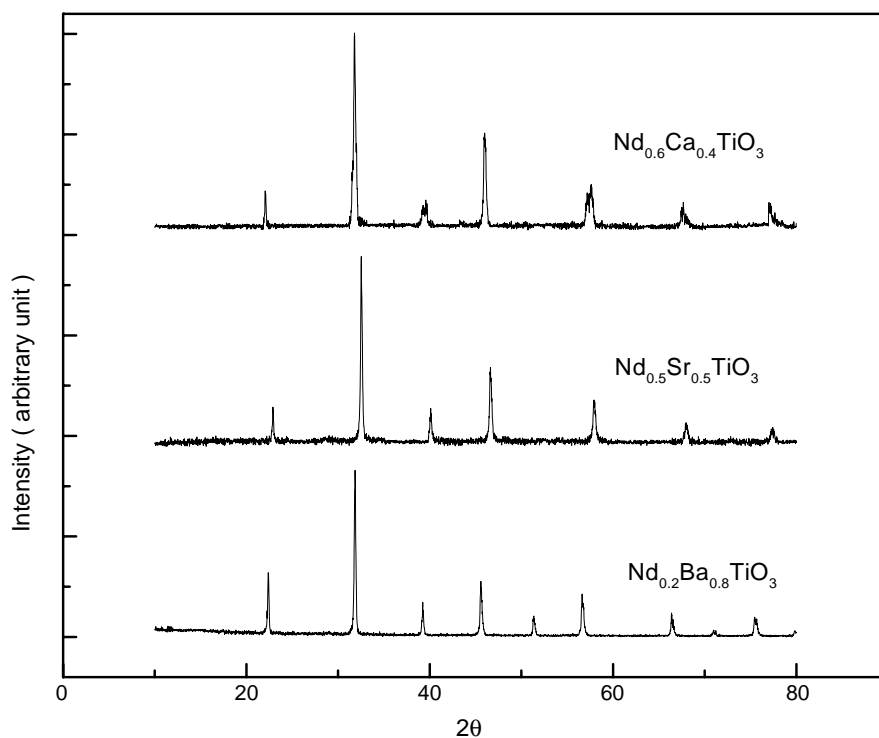


Fig. 1. X-ray diffraction pattern of  $\text{Nd}_{0.6}\text{Ca}_{0.4}\text{TiO}_3$ ,  $\text{Nd}_{0.5}\text{Sr}_{0.5}\text{TiO}_3$  and  $\text{Nd}_{0.2}\text{Ba}_{0.8}\text{TiO}_3$ .

( $x \leq 0.1$ ) shows semiconducting like behavior whereas those with  $x \geq 0.2$  exhibit metallic properties. This result suggests that a transition from insulator to metal (I–M) should occur in the range  $x = 0.1$ – $0.2$ . Furthermore partial

replacement of Nd by Ca convert the Mott–Hubbard insulator  $\text{NdTiO}_3$  ( $x = 0$ ) with  $3d^1$  configuration to a metallic state thereby resulting to a M–I transition near  $x \sim 0.15$  [21].

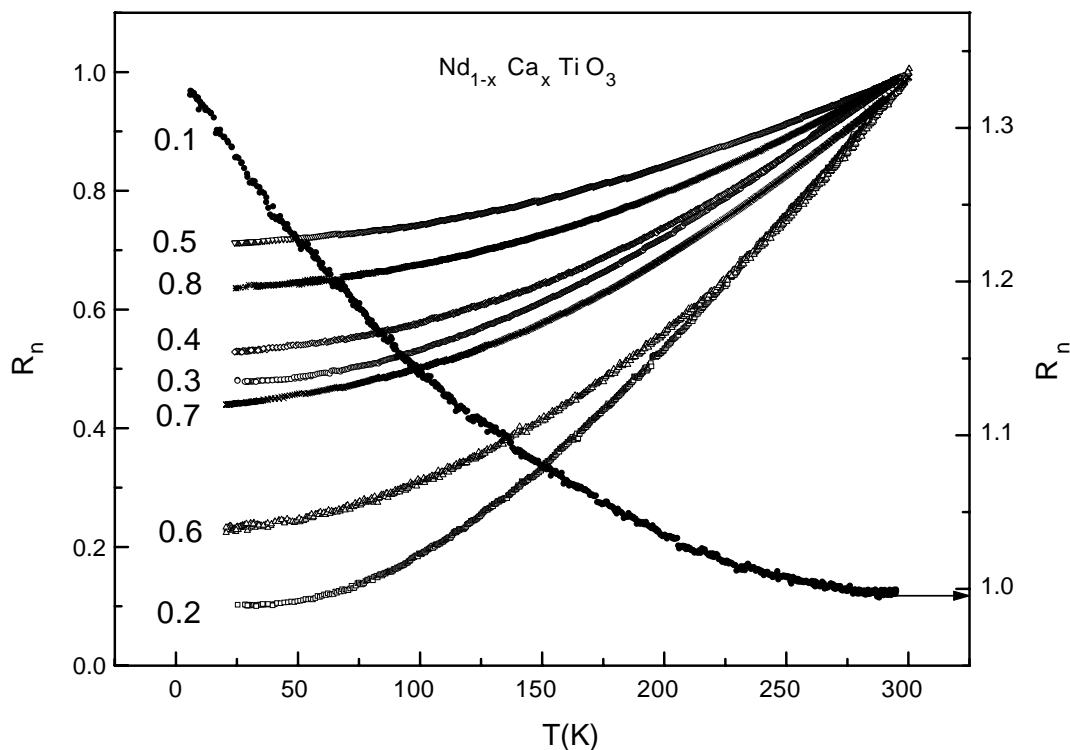


Fig. 2. The temperature dependence of the normalized resistance  $R_n (=R/R_{300})$  for  $\text{Nd}_{1-x}\text{Ca}_x\text{TiO}_3$  ( $x = 0.1$ – $0.8$ ).

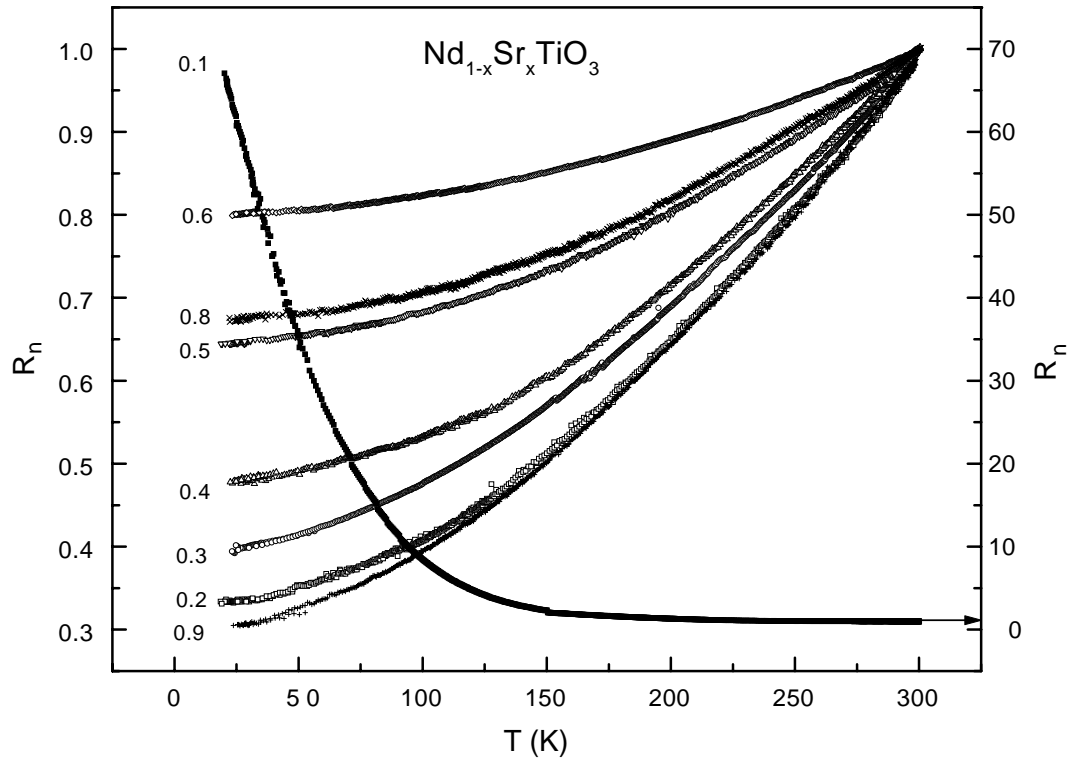


Fig. 3. Plot of  $R_n$  as a function of temperature for  $\text{Nd}_{1-x}\text{Sr}_x\text{TiO}_3$  ( $x = 0.1-0.9$ ).

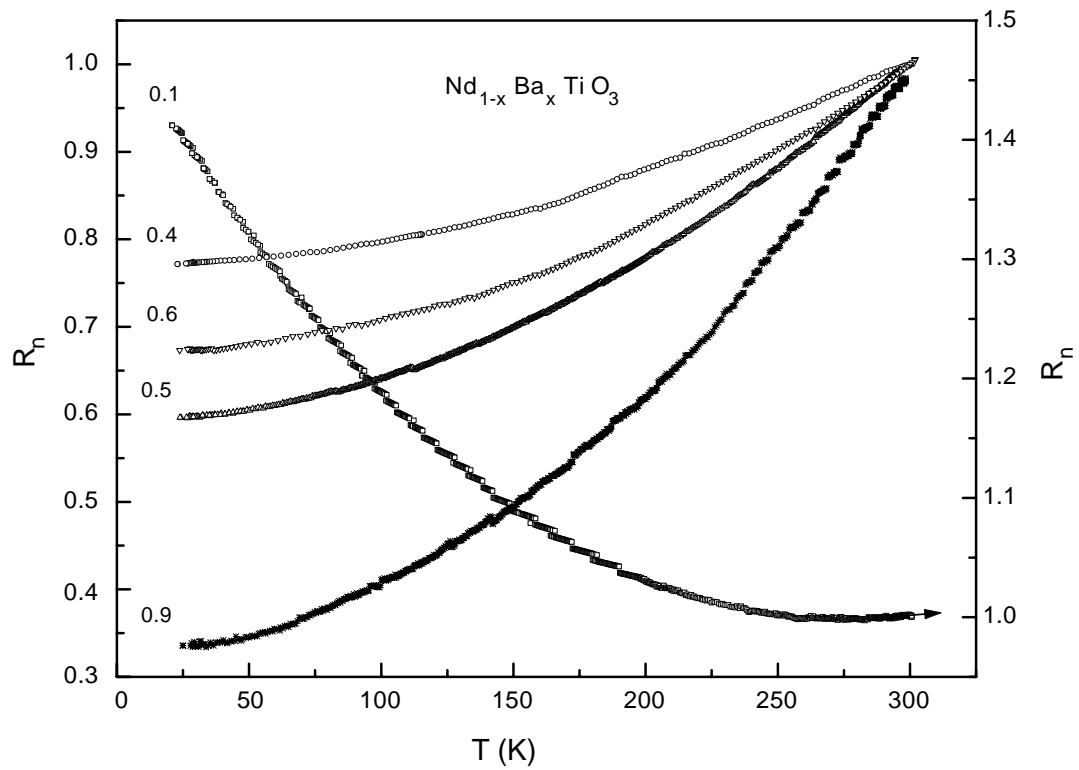


Fig. 4. Thermal variation of  $R_n$  of  $\text{Nd}_{1-x}\text{Ba}_x\text{TiO}_3$  ( $x = 0.1-0.9$ ).

The variation of  $R_n$  as a function of temperature in  $\text{Nd}_{1-x}\text{Sr}_x\text{TiO}_3$  ( $x = 0.1\text{--}0.9$ ) is shown in Fig. 3. Here also we have noticed that with replacement of Nd by Sr the functional dependence of  $R_n$  follows a similar fashion as that observed in  $\text{Nd}_{1-x}\text{Ca}_x\text{TiO}_3$ . For example,  $x = 0.1$  sample shows semiconducting behavior whereas samples with  $x \geq 0.2$  exhibits metallic nature. From the functional dependence of the resistivity with temperature it appears that in this case the insulator-metal transition occurs in between  $x = 0.15$  and  $x = 0.2$  [22].

In Fig. 4 we show plots of  $R_n$  as a function of temperature for the  $\text{Nd}_{1-x}\text{Ba}_x\text{TiO}_3$  ( $x = 0.1\text{--}0.9$ ) series. For  $x = 0.1$ ,  $R_n$  increases with decrease of temperature like a semiconducting material. Similar semiconducting type of electrical transport has also been observed in other titanate systems in the vicinity of the parent insulating state. Moreover, as one approaches the insulating state from the metallic side the carrier effective mass is found [18] to be critically enhanced owing to the electron correlation effect. Observation of the insulating state with finite doping may be ascribed to the carrier localization effect arising from a combined effect of the correlation enhanced effective mass and the random potential induced from the ionic A-sites of the  $\text{ABO}_3$  perovskite structure (Nd/Ba mixture). For  $x > 0.1$ ,  $R_n(T)$  shows metallic behavior as observed in Ca- and Sr-doped  $\text{NdTiO}_3$  systems mentioned above.

In the metallic regime of  $\text{Nd}_{1-x}\text{A}_x\text{TiO}_3$  ( $A = \text{Ca, Sr and Ba}$ ) we have observed that the temperature dependence

of  $R_n$  can be described quite satisfactorily by the relation  $R_n = R_{n0} + AT^2$ , where  $R_{n0}$  is the residual normalized resistance and  $A$  is a constant. In order to determine the nature of metallicity we have plotted  $R_n$  as a function of  $T^2$  in Fig. 5 for  $\text{Nd}_{1-x}\text{A}_x\text{TiO}_3$  ( $A = \text{Ca and Sr}$ ) over a temperature range 20–300 K. In the case of Ba-doped  $\text{NdTiO}_3$  we also observed a similar type of  $T^2$  dependence for  $R_n$ . For all the compounds the linear nature of the curve suggests that strong electron–electron scattering plays an important role in governing the electrical conduction in these materials. This  $T^2$  behavior of  $R_n$  is one of the characteristic fingerprints of a Fermi liquid [23,24]. In the metallic  $\text{Nd}_{1-x}\text{Ca}_x\text{TiO}_3$  compounds it has been reported [21] that the effective mass of the carrier increases as the M–I boundary ( $x = 0.15$ ) is approached.

From the above discussions on the variation of resistance with temperature in  $\text{Nd}_{1-x}\text{A}_x\text{TiO}_3$  ( $A = \text{Ca, Sr and Ba}$ ) as a function of 3d conduction band filling  $n$  ( $=1 - x$ ) we may arrive at the following results. Partial substitution of Nd with divalent alkaline-earth A ions (Ca, Sr and Ba) transforms the Mott–Hubbard insulator  $\text{NdTiO}_3$  with  $3d^1$  configuration into a correlated metal thereby leading to an insulator-metal transition. However, depending upon the size of the dopant ion A, the M–I transition occurs at different levels of band filling. For instance when the size of the A ion is large (e.g., Ba), a 20% Ba substitution is sufficient to induce the M–I transition in  $\text{NdTiO}_3$  whereas for dopants of smaller size (e.g., Sr and Ca) it takes place at 20% Sr substitution and

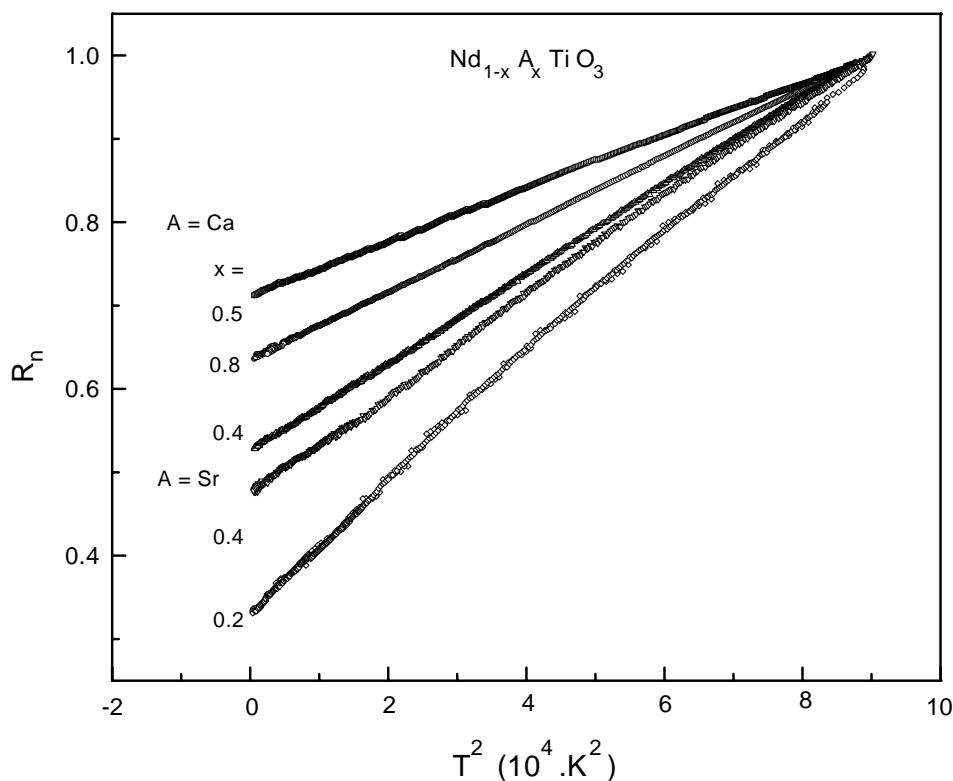


Fig. 5. Variation of  $R_n$  as a function of  $T^2$  for  $\text{Nd}_{1-x}\text{A}_x\text{TiO}_3$  ( $A = \text{Ca; } x = 0.4, 0.5, 0.8$  and  $A = \text{Sr; } x = 0.2, 0.4$ ).

15% Ca substitution, respectively. This result is consistent with our recent observation [25] in the strongly correlated  $Y_{1-x}A_xTiO_3$  ( $A = Ca, Sr$  and  $Ba$ ) where also the 3d band filling level ( $x$ ) for the occurrence of M–I transition depends on the size of the A-ion. For  $A = Ca$ ,  $YTiO_3$  requires a higher hole doping (40% Ca) while for  $A = Sr$  or  $Ba$ , it requires comparatively less hole doping (35% Sr or, 20% Ba) to induce the M–I transition. It is to be mentioned here that a  $\sim 5\%$  Sr substitution is sufficient to induce the metallic phase in the weakly correlated  $LaTiO_3$  [14]. Thus  $NdTiO_3$  which is intermediate between  $LaTiO_3$  and  $YTiO_3$ , requires a lower amount of substitution of A for Nd than in the strongly correlated  $YTiO_3$  to induce the M–I transition. A systematic investigation of the electronic properties in  $Nd_{1-x}Ca_xTiO_3$ ,  $La_{1-x}Sr_xTiO_3$  [14] and  $Y_{1-x}Ca_xTiO_3$  [16] systems reveals that on the verge of the M–I transition the carrier effective mass increases. Furthermore, on approaching the I–M phase from the metallic side the observed enhancement of the carrier effective mass may be due to the filling dependent change of the correlation effect. In the vicinity of the M–I transition the combined effect of the correlation enhanced effective mass and the random potential arising from the perovskite A-sites gives rise to localization of charge carriers. The Fermi liquid type behaviors observed in the correlated metallic phase seems to be a common features of the divalent alkaline earth ion doped titanate systems.

### 3.3. Thermoelectric power

Thermoelectric effects which are responsible for the direct conversion of heat energy into electrical energy and vice

versa have recently received new interest in the thermopower of correlated materials. Thermoelectric power (TEP,  $S$ ) is a very useful probe to study the semiconducting and metallic behavior of compounds since it offers a characteristic difference in the two cases. We have measured the TEP of  $Nd_{1-x}A_xTiO_3$  ( $A = Ca, Sr$  and  $Ba$ ) in the correlated metallic phase. The metallic TEP has a low value at room temperature and varies linearly with temperature. The sign of the TEP describes (not always) the type of majority carriers present in the compound at a certain temperature.

In Fig. 6 we present the temperature variation of  $S$  in  $Nd_{1-x}Ca_xTiO_3$  ( $x = 0.2–0.9$ ). For all the samples  $S$  is found to be negative indicating electronic charge carriers. Fig. 6 shows that  $S$  varies linearly with temperature irrespective of the 3d conduction band filling level. This is consistent with the observed correlated metallic behavior of the electrical transport in this range of band filling. Thermal variation of  $S$  for  $Nd_{1-x}Sr_xTiO_3$  ( $x = 0.3–0.8$ ) and  $Nd_{1-x}Ba_xTiO_3$  ( $x = 0.1–0.8$ ) for different band filling are shown in Figs. 7 and 8, respectively. Both the systems exhibit  $S(T)$  curves which are quite similar in nature to those observed in  $Nd_{1-x}Ca_xTiO_3$ .

It is to be pointed out here that monovalent metals, noble metals and some other metals [26] also exhibit a linear dependence of  $S$  on  $T$  similar to that observed in doped titanate oxides mentioned above. Considering the nearly free electron model, Mott [27] has given an expression for the characteristic diffusion thermopower of a metal as

$$S(T) = \left( \frac{\pi^2 k_B^2 T}{3e} \right) \left[ \frac{d(\ln \sigma(E))}{dT} \right]_{E=E_F} \quad (1)$$

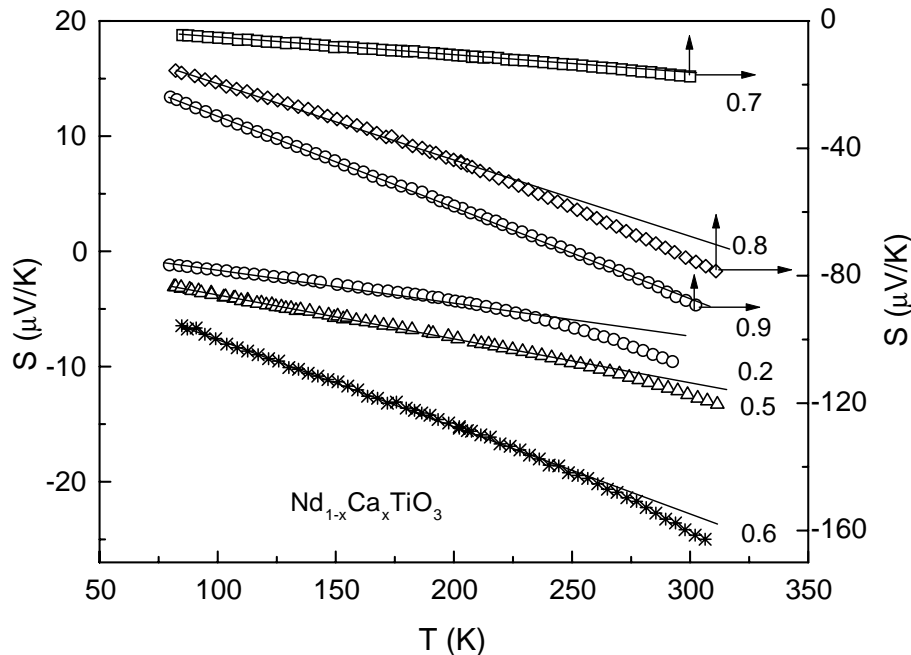


Fig. 6. The temperature dependence of the thermopower ( $S$ ) of  $Nd_{1-x}Ca_xTiO_3$  for different  $x$ . Solid line represents the theoretical fit following the expression (3) described in the text.

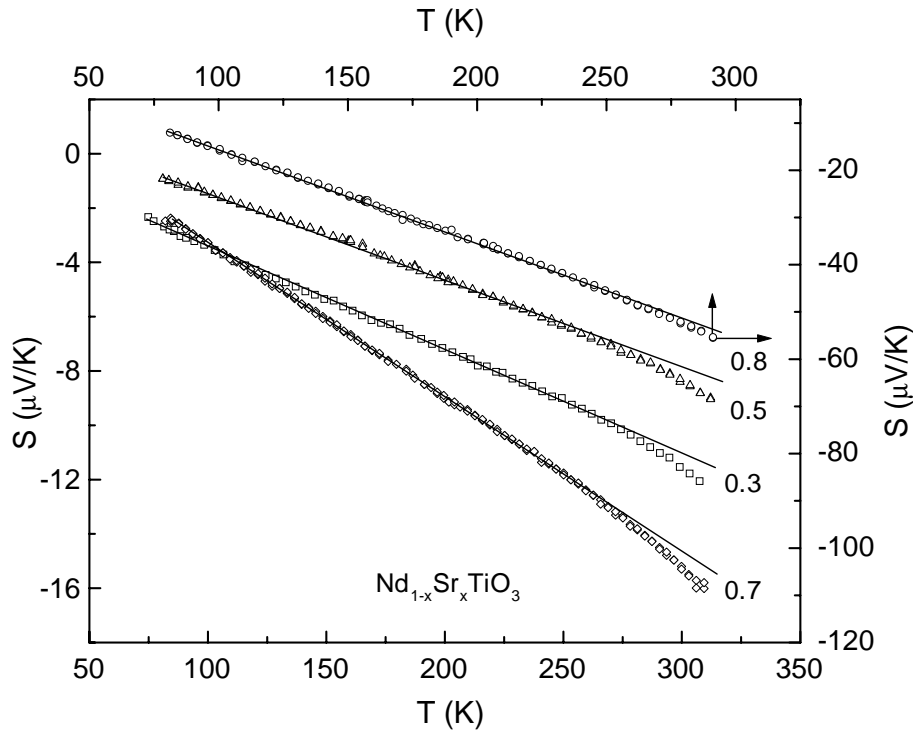


Fig. 7. Plot of  $S$  as a function of temperature for  $\text{Nd}_{1-x}\text{Sr}_x\text{TiO}_3$  along with the fitted curve (solid line).

where  $k_B$  is Boltzmann's constant,  $E_F$  the Fermi energy and  $e$  is the charge of the carriers. Assuming that the conductivity is proportional to the energy and that there is a  $T$ -independent mean free path for the carriers, expression (1) becomes

$$S(T) \approx \frac{\pi^2 k_B^2 T}{3eE_F} \quad (2)$$

Eq. (2) is derived considering a spherical Fermi surface together with a  $T$ -independent relaxation. This approximation limits the validity of Eq. (2) to low temperatures. From the above relation  $S$  is linear with  $T$  and is extremely sensitive on the nature of the Fermi surface. Experimental data belonging to the linear region of the  $S(T)$  curve for  $\text{Nd}_{1-x}\text{A}_x\text{TiO}_3$  ( $A = \text{Ca}, \text{Sr}$  and  $\text{Ba}$ ) can be fitted quite satisfactorily

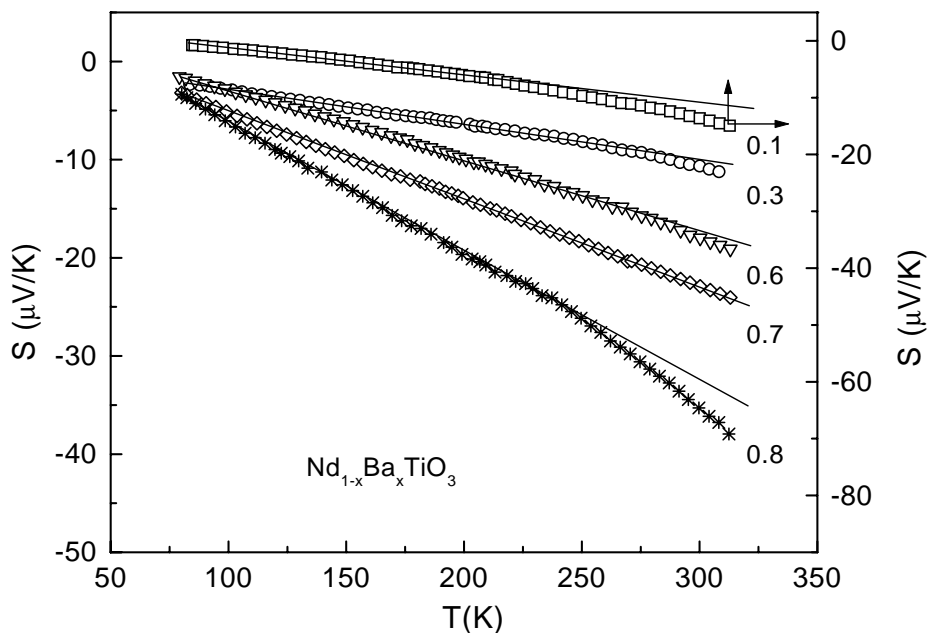


Fig. 8. Thermal dependence of  $S$  for  $\text{Nd}_{1-x}\text{Ba}_x\text{TiO}_3$ . Solid line is the fitted curve.

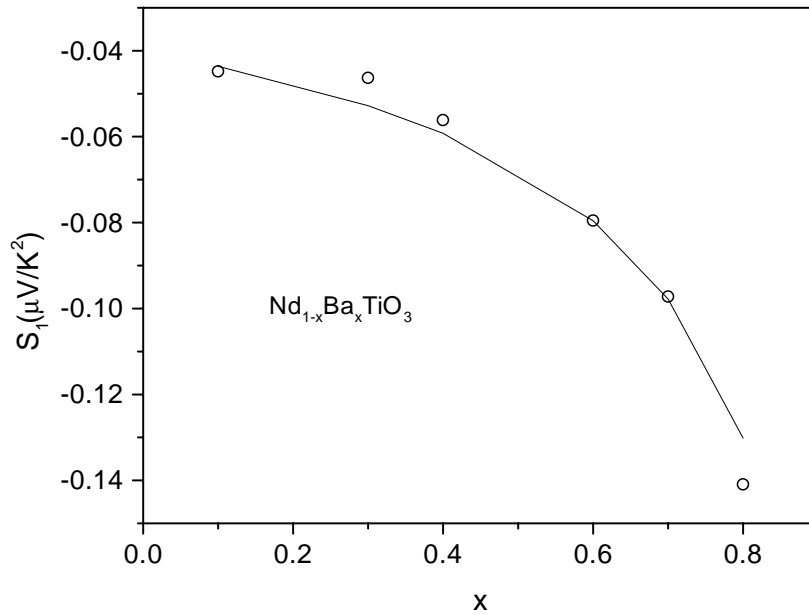


Fig. 9. Variation of the coefficient  $S_1$  as a function of the filling level ( $x$ ) for  $\text{Nd}_{1-x}\text{Ba}_x\text{TiO}_3$ .

considering the expression

$$S(T) = S_0 + S_1 T \quad (3)$$

and the fit is shown by solid lines in Figs. 6–8, respectively. Here  $S_0$  ( $=S$  at  $T = 0$ ) can be obtained from the extrapolation of the high temperature fit of  $S$ . This term has no physical origin and is inserted to overcome the problem of truncating the low temperature data. Thus from the slope of the  $S(T)$  curve one can obtain knowledge about how  $S_1$  varies with filling level ( $x$ ). In Fig. 9 we have plotted  $S_1$  as a function of  $x$  for  $\text{Nd}_{1-x}\text{Ba}_x\text{TiO}_3$ . Now comparing Mott's relation (2) with expression (3), the coefficient  $S_1$  of the  $T$  linear term can be written as  $S_1 = \pi^2 k_B^2 / 3eE_F$ . According to the free electron theory  $E_F$  is given by  $E_F = \hbar^2 / 2m^* (3\pi^2 n_f)^{2/3}$ , where  $\hbar = h/2\pi$ ,  $h$  being Planck's constant,  $m^*$  the effective mass and  $n_f$  is the free electron density. Theoretical estimations of  $n_f$  have been made using values of the mass density obtained from X-ray diffraction data under the assumption of four formula units per cell [28]. For the Ba-doped samples,  $n_f$  is taken as  $1.615 \times 10^{22}(1-x)$ . The best theoretical fit to the experimentally evaluated  $S_1$  versus  $x$  data (open symbol) obtained with  $m^* = 5m_0$  (where  $m_0$  is the free electron mass) is shown in Fig. 9 by solid line. Such an enhancement of mass ( $m^*/m \sim 10$ ) has also been reported [21] from the analysis of the resistivity data of  $\text{Nd}_{0.4}\text{Ca}_{0.6}\text{TiO}_3$ . Similar enhancement in the effective mass of the charge carriers has been obtained by analyzing the thermoelectric power data in  $\text{La}_{1-x}\text{Sr}_x\text{TiO}_3$  [29] and  $\text{Y}_{1-x}\text{A}_x\text{TiO}_3$  ( $A = \text{Ca}, \text{Sr}$  and  $\text{Ba}$ ) [25]. In  $\text{La}_{1-x}\text{Sr}_x\text{TiO}_3$  Tokura et al. [14] observed an increase of the  $T$ -linear term in the low temperature specific heat with band filling indicating an enhancement of the effective mass. Thus the oc-

currence of the observed MI transition is associated with an enhancement of the effective mass of the carriers caused by the strong correlation effects. In our case a very simplified model for the thermopower also indicates a mass enhancement though the factor of enhancement obtained by other experimental techniques is higher. It is felt that for a true analysis of the thermopower data a very precise expression for  $S$  is needed on the basis of the actual band structure.

#### 4. Conclusion

Analysis of the X-ray data reveals that  $\text{NdTiO}_3$  doped with Ca and Sr belongs to the orthorhombic structure and when doped with Ba shows cubic symmetry. Analysis of the electrical transport of  $\text{Nd}_{1-x}\text{A}_x\text{TiO}_3$  ( $A = \text{Ca}, \text{Sr}$  and  $\text{Ba}$ ) suggests that for all the compounds the nature of charge conduction depends sensitively on the 3d band filling level  $n$  ( $=1-x$ ). For each compound as the filling level varies the electrical conduction changes from insulating to metallic type leading to a M–I transition. Moreover, the filling level at which the insulator-metal transition occurs depends on the size of the divalent alkaline earth A-ion. In the correlated metallic phase the Fermi liquid description seems to be a common feature of the divalent alkaline earth-ion doped titanate systems. In this regime of filling, the electrical transport data indicates that the electron–electron scattering plays a major role governing the conduction process. Analysis of the TEP data belonging to the linear region of the  $S(T)$  curve reveals an enhancement of the carrier effective mass.

## References

- [1] N.F. Mott, *Metal-Insulator Transition*, second ed., Taylor and Francis, London, 1990.
- [2] M. Imada, A. Fujimori, Y. Tokura, *Rev. Mod. Phys.* 70 (1998) 1039.
- [3] J. Zaanen, G.A. Sawatzky, J.W. Allen, *Phys. Rev. Lett.* 55 (1985) 418.
- [4] D.B. Mc Whan, J.P. Remeika, T.M. Rice, W.F. Brinkman, J.P. Maita, A. Menth, *Phys. Rev. Lett.* 27 (1971) 941; D.P. Mc Whan, A. Menth, J.P. Remeika, W.F. Brinkman, T.M. Rice, *Phys. Rev.* B7 (1973) 1920.
- [5] P.C. Canfield, J.D. Thompson, S.-W. Cheong, L.W. Rupp, *Phys. Rev.* B47 (1993) 12357.
- [6] J.B. Torrance, P. Lacorro, A.I. Nazzal, E.J. Ansaldo, Ch. Niedermayer, *Phys. Rev.* B45 (1992) 8209.
- [7] C.N.R. Rao, A. Arulraj, A.K. Cheetham, B. Raveau, *J. Phys. Condens. Matter* 12 (2000) R83.
- [8] J.M.D. Coey, M. Virret, S. von Molnar, *Adv. Phys.* 48 (2) (1999) 167.
- [9] A.P. Ramirez, *J. Phys. Condens. Matter* 9 (1997) 81711.
- [10] R. Vijayraghavan, L.C. Gupta, *Int. J. Mod. Phys.* 9 (1995) 633.
- [11] J.G. Bednorz, K.A. Muller, *Z. Phys. B* 64 (1986) 189.
- [12] E. Dagotto, *Rep. Prog. Phys.* 62 (1999) 1525.
- [13] H. Suzuki, H. Bando, Y. Ootuka, I.H. Inoue, T. Yamamoto, K. Takahashi, Y. Nishihara, *J. Phys. Soc. Japan* 65 (1996) 1529.
- [14] Y. Tokura, T. Taguchi, Y. Okada, Y. Fujishima, T. Arima, K. Kumagai, Y. Iye, *Phys. Rev. Lett.* 70 (1993) 2126.
- [15] F. Lichtenberg, D. Widmer, J.G. Bednorz, T. Williams, A. Reller, *Z. Phys.* B84 (1991) 369; Y. Okada, T. Arima, Y. Tokura, C. Murayama, N. Mori, *Phys. Rev.* B48 (1993) 9677.
- [16] Y. Taguchi, Y. Tokura, T. Arima, F. Inaba, *Phys. Rev.* B48 (1993) 511.
- [17] Y. Okimoto, T. Katsufuji, Y. Okada, T. Arima, Y. Tokura, *Phys. Rev.* B51 (1995) 9581.
- [18] K. Kumagai, T. Suzuki, Y. Taguchi, Y. Okada, Y. Fujishima, Y. Tokura, *Phys. Rev.* B48 (1993) 7636.
- [19] Y. Tokura, T. Taguchi, Y. Moritomo, K. Kumagai, T. Suzuki, Y. Iye, *Phys. Rev.* B48 (1993) 14063.
- [20] R. Gangopadhyay, A. De, S. Das, *J. Appl. Phys.* 87 (2000) 2363.
- [21] H.L. Ju, C. Eylem, J.L. Peng, B.W. Eichhorn, R.L. Greene, *Phys. Rev.* B49 (1994) 13335.
- [22] C. Eylem, H.L. Ju, B.W. Eichhorn, R.L. Greene, *J. Solid State Chem.* 114 (1995) 164.
- [23] P. Nozieres, *Theory of Interacting Fermi Systems*, W.A. Benjamin Inc., New York, 1964.
- [24] D. Pines, P. Nozieres, *The Theory of Quantum Liquids*, vol. 1, W.A. Benjamin Inc., New York, 1966.
- [25] S. Das, A. Poddar, B. Roy, *J. Alloys Compd.* 358 (2003) 17.
- [26] F.J. Blatt, P.A. Schroeder (Eds.), *Thermoelectricity in Metallic Conductors*, Plenum Press, New York, 1958, p. 310.
- [27] N.F. Mott, H. Jones, *The Theory of the Properties of Metals and Alloys*, Dove Publications Inc., New York, 1958, p. 310.
- [28] D.A. Maclean, N.G. Hok-Nam, J.E. Greedan, *J. Solid State Chem.* 30 (1979) 35.
- [29] M. Onoda, M. Kohno, *J. Phys. Condens. Matter.* 10 (1998) 1003.